The Astrophysical Journal Letters, 770:L17 (6pp), 2013 June 20 doi:10.1088/2041-8205/770/2/L17

A PECULIAR FAINT SATELLITE IN THE REMOTE OUTER HALO OF M31*

A. D. Mackey[1], A. P. Huxor[2], N. F. Martin[3,4], A. M. N. Ferguson[5], A. Dotter[1], A. W. McConnachie[6], R. A. Ibata[3], M. J. Irwin[7], G. F. Lewis[8], C. M. Sakari[9], N. R. Tanvir[10], and K. A. Venn[9]
[1] Research School of Astronomy & Astrophysics, The Australian National University, Mount Stromlo Observatory, via Cotter Road, Weston, ACT 2611, Australia; dougal@mso.anu.edu.au
[2] Astronomisches Rechen-Institut, Universität Heidelberg, Mönchhofstraße 12-14, D-69120 Heidelberg, Germany
[3] Observatoire astronomique de Strasbourg, Université de Strasbourg, CNRS, UMR 7550, 11 rue de l'Université, F-67000 Strasbourg, France
[4] Max-Planck-Institut für Astronomie, Königstuhl 17, D-69117 Heidelberg, Germany
[5] Institute for Astronomy, University of Edinburgh, Royal Observatory, Blackford Hill, Edinburgh EH9 3HJ, UK
[6] NRC Herzberg Institute for Astrophysics, 5071 West Saanich Road, Victoria, BC V9E 2E7, Canada
[7] Institute of Astronomy, University of Cambridge, Madingley Road, Cambridge CB3 0HA, UK
[8] Sydney Institute for Astronomy, School of Physics, A28, The University of Sydney, NSW 2006, Australia
[9] Department of Physics & Astronomy, University of Victoria, 3800 Finnerty Road, Victoria, BC V8P 1A1, Canada
[10] Department of Physics and Astronomy, University of Leicester, University Road, Leicester LE1 7RH, UK
Received 2013 April 17; accepted 2013 April 29; published 2013 May 30

ABSTRACT

We present *Hubble Space Telescope* imaging of a newly discovered faint stellar system, PAndAS-48, in the outskirts of the M31 halo. Our photometry reveals this object to be comprised of an ancient and very metal-poor stellar population with age $\gtrsim$10 Gyr and [Fe/H] $\lesssim -2.3$. Our inferred distance modulus $(m - M)_0 = 24.57 \pm 0.11$ confirms that PAndAS-48 is most likely a remote M31 satellite with a three-dimensional galactocentric radius of 149^{+19}_{-8} kpc. We observe an apparent spread in color on the upper red giant branch that is larger than the photometric uncertainties should allow, and briefly explore the implications of this. Structurally, PAndAS-48 is diffuse, faint, and moderately flattened, with a half-light radius $r_h = 26^{+4}_{-3}$ pc, integrated luminosity $M_V = -4.8 \pm 0.5$, and ellipticity $\epsilon = 0.30^{+0.08}_{-0.15}$. On the size–luminosity plane it falls between the extended globular clusters seen in several nearby galaxies and the recently discovered faint dwarf satellites of the Milky Way; however, its characteristics do not allow us to unambiguously classify it as either type of system. If PAndAS-48 is a globular cluster then it is among the most elliptical, isolated, and metal-poor of any seen in the Local Group, extended or otherwise. Conversely, while its properties are generally consistent with those observed for the faint Milky Way dwarfs, it would be a factor of ∼2–3 smaller in spatial extent than any known counterpart of comparable luminosity.

Key words: galaxies: dwarf – galaxies: individual (M31) – globular clusters: general – Local Group

Online-only material: color figures

1. INTRODUCTION

In recent years, the advent of deep wide-field sky surveys has heralded the discovery of a variety of new and unusual diffuse stellar systems in the Local Group. Arguably, the most significant of these are the ultra-faint dwarf (UFD) satellites of the Milky Way (e.g., Willman et al. 2005; Zucker et al. 2006; Belokurov et al. 2007), the existence of which may have important implications for the "missing satellites" problem of ΛCDM cosmology (e.g., Koposov et al. 2009). These objects have luminosities as low as $M_V \sim -1.5$, and, with characteristic radii commonly in the range $r_h \sim$ 25–100 pc (e.g., Martin et al. 2008; Sand et al. 2012), physical sizes that are substantially smaller than those of classical dwarf spheroidal galaxies and which, in some cases, approach the globular cluster (GC) regime.

UFDs have two key characteristics distinguishing them as galaxies. First, although analysis of their internal kinematics is fraught with complexity due to, for example, the presence of binary stars and the effects of external tidal forces (e.g., McConnachie & Côté 2010; Simon et al. 2011), radial velocity observations consistently imply mass-to-light ratios as high as a few thousand (e.g., Martin et al. 2007; Simon & Geha 2007). Second, their constituent stellar populations (1) are ancient and very metal-poor with $\langle$[Fe/H]$\rangle \lesssim -2.2$ (e.g., Kirby et al. 2011; Brown et al. 2012); (2) frequently exhibit substantial internal dispersions in iron abundance of up to ∼0.6–0.7 dex (e.g., Martin et al. 2007; Kirby et al. 2008); and (3) sometimes include extremely metal-poor members with [Fe/H] < -3 (e.g., Norris et al. 2010). UFDs apparently extend the metallicity–luminosity relation seen for classical Milky Way satellites (e.g., Kirby et al. 2011), suggesting that they are not the stripped remnants of once-larger progenitors (see also Leaman 2012).

A second recently discovered class of diffuse stellar systems is that of the so-called extended clusters (ECs; Huxor et al. 2005). These provoked interest because the first luminous examples appeared isolated on the size–luminosity plane, encroaching upon the empty region separating GCs from dwarf galaxies. However, subsequent work uncovered many fainter ECs in M31 (Huxor et al. 2008) and other Local Group galaxies (Stonkutė et al. 2008; Huxor et al. 2009, 2013; Hwang et al. 2011), and these fill out a region on the plane with $-8 \lesssim M_V \lesssim -5$ and $r_h \sim$ 15–35 pc that overlaps substantially with the most diffuse GCs seen in the Milky Way (Huxor et al. 2011). Along with refined structural measurements (Tanvir et al. 2012) and resolved photometry precluding large internal spreads in [Fe/H] (Mackey et al. 2006), this suggests that ECs most likely represent the upper tail of the GC size distribution (see also Da Costa et al. 2009). It remains to be convincingly demonstrated kinematically that ECs need not contain any dark matter component

* Based on observations made with the NASA/ESA *Hubble Space Telescope*, obtained at the Space Telescope Science Institute (STScI), which is operated by the Association of Universities for Research in Astronomy, Inc., under NASA contract NAS 5-26555. These observations are associated with program GO 12515.

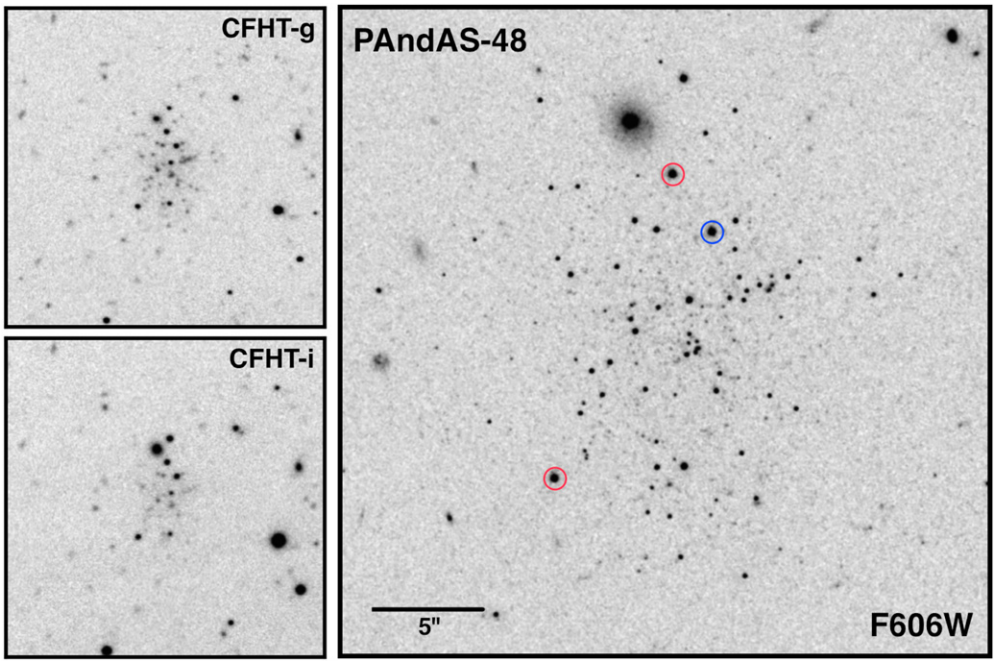

Figure 1. Left panels: PA-48 discovery images, 1′ on a side, in the CFHT/MegaCam *g* and *i* bands. Right panel: our 30″ × 30″ drizzled F606W ACS/WFC image of PA-48. Star-A and star-C from Section 3.1 are circled in red; star-B in blue. North is to the top and east to the left in all images.

(A color version of this figure is available in the online journal.)

(e.g., Collins et al. 2009), but they nonetheless apparently stand clearly distinct from UFDs despite their close proximity on the size–luminosity plane.

M31 is an excellent location for studying a wide variety of stellar systems, as it possesses many more dwarf satellites (e.g., McConnachie 2012) and GCs (e.g., Galleti et al. 2004) than does the Milky Way. Recently, we have conducted the Pan-Andromeda Archaeological Survey (PAndAS; McConnachie et al. 2009), imaging the M31 halo to a projected galactocentric distance of $R_p \approx 150$ kpc with CFHT/MegaCam and facilitating the first detailed characterization of this region and the star clusters and dwarf galaxies that inhabit it (e.g., Huxor et al. 2008; McConnachie et al. 2008; Richardson et al. 2011).

One of the most intriguing of our discoveries is PAndAS-48 (PA-48), at $\alpha = 00^{\rm h}59^{\rm m}28\overset{\rm s}{.}3$, $\delta = +31^{\circ}29'10\overset{''}{.}6$ (J2000), which we uncovered during our search for remote GCs in M31 (A. P. Huxor et al. 2013, in preparation). This is a very faint stellar system with $M_V \approx -4.7$ lying at $R_p = 141$ kpc. The PAndAS discovery images (Figure 1) reveal a notably elongated object with a very diffuse structure. In this Letter, we present deep *Hubble Space Telescope* (*HST*) follow-up imaging of PA-48 and show that, unusually, it possesses characteristics that do not allow it to be unambiguously classified as either an EC or a faint dwarf galaxy.

2. OBSERVATIONS AND DATA ANALYSIS

We observed PA-48 with the Wide Field Channel (WFC) of the Advanced Camera for Surveys (ACS) aboard *HST* on 2011 November 3 as part of program GO 12515 (PI: Mackey). The object was imaged three times in both the F606W and F814W filters, with small dithers between exposures. Integration times were 799 s for F606W frames and 845 s for F814W frames.

We obtained the reduced data from the *HST* archive. The CALACS pipeline now includes a pixel-based charge-transfer efficiency (CTE) correction (e.g., Anderson & Bedin 2010) as well as improved corrections for effects introduced by the ACS electronics. In the right panel of Figure 1, we display the drizzled, CTE-corrected F606W image of PA-48. The object is fully resolved, and we confirm it as a faint, low surface brightness stellar system with an extended structure; the apparently elongated morphology persists.

We photometered our images using version 2.0 of the DOLPHOT photometry software (Dolphin 2000). DOLPHOT performs point-spread function (PSF) fitting using model PSFs especially tailored to the ACS/WFC camera. The software provides a variety of photometric quality parameters for each detection. We selected those objects classified as stellar, with valid photometry in all six input images, a global sharpness parameter between ±0.1 in each filter, and a crowding parameter ⩽0.08 mag in each filter. Our final photometry is on the calibrated VEGAMAG scale of Sirianni et al. (2005).

We assessed the photometric uncertainties and detection completeness by performing artificial star tests. For each real star, we randomly generated 500 artificial stars of the same brightness but with positions uniformly distributed within a radius $1'' \leqslant r \leqslant 5''$ of its coordinates. DOLPHOT adds a single artificial star at a time to the images and then attempts to measure it. We filtered the results according to the photometric quality parameters as described above, and for each real star (1) assigned a detection completeness by comparing the number of recovered objects with the number submitted and (2) characterized the photometric uncertainties by examining the scatter in the differences between the input and measured magnitudes of the artificial stars. Our 50% completeness level is at $m_{\rm F606W} = 27.5$ and $m_{\rm F814W} = 26.8$, where the uncertainties are typically ±0.1 mag in both filters.

3. RESULTS

3.1. Color–Magnitude Diagram

Figure 2 shows our color–magnitude diagram (CMD) for PA-48. We observe a steep red giant branch (RGB) and a blue

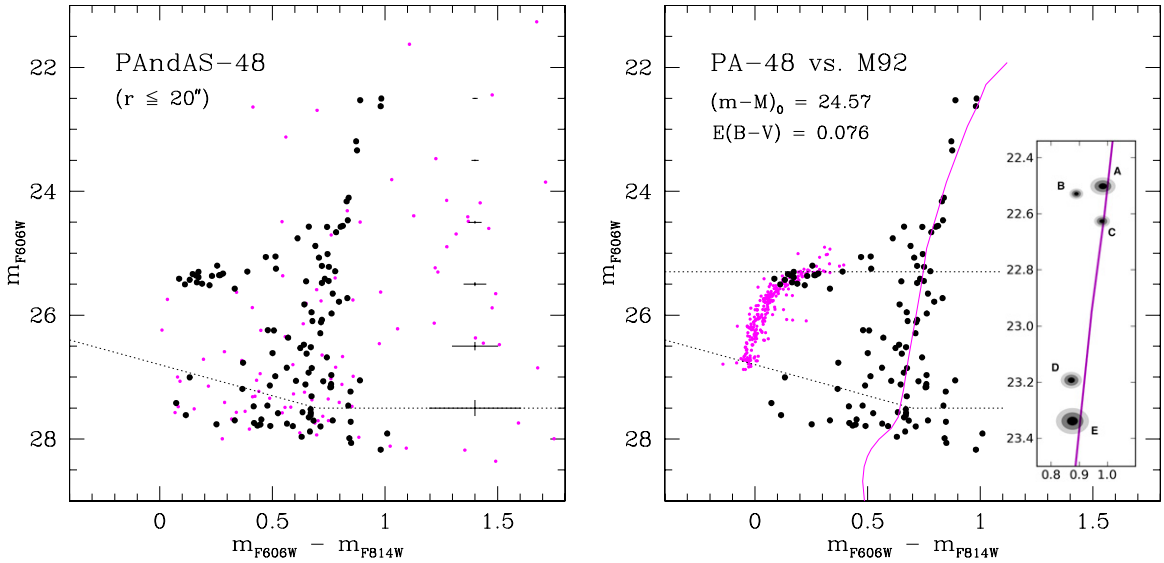

Figure 2. Left panel: our ACS/WFC CMD for PA-48. Field stars more than 50″ away from the cluster center are marked with small magenta points. The dotted line is our 50% completeness level. Right panel: the PA-48 CMD with registered M92 fiducial and HB. The inset shows stars on the upper RGB with individual 1σ, 2σ, and 3σ photometric uncertainties. The five brightest stars are labeled A–E.

(A color version of this figure is available in the online journal.)

horizontal branch (HB), characteristic of the ancient ($\gtrsim$10 Gyr old) stellar populations seen in both GCs and low-luminosity dwarfs. At the top of the RGB, there is the suggestion of a spread in color that is larger than the photometric uncertainties should allow; we discuss this in more detail below.

To obtain a photometric metallicity estimate for PA-48, we aligned de-reddened GC fiducials from Brown et al. (2005), following the procedures described in Mackey et al. (2006, 2007). Briefly, we registered the fiducials using the observed level of the HB and the color of the RGB at the HB level. The metallicity sets the curvature of the upper RGB. Because PA-48 is in the remote halo of M31, it may not lie at the same distance as the galaxy's center. For each fiducial, we therefore tested distance moduli in a range ±0.5 mag about the usual $(m-M)_0 = 24.47$ for M31. At given $(m-M)_0$, we calculated the foreground extinction necessary to align the HB levels of the CMD and the reference fiducial. This in turn allowed us to calculate the offset in color between the CMD and fiducial RGB sequences at the HB level. The best combination of $(m-M)_0$ and $E(B-V)$ for a given fiducial was that which minimized this offset. We then examined how closely the shapes of the CMD and fiducial RGB sequences matched.

The most metal-poor cluster in the Brown et al. (2005) sample—M92, with [Fe/H] ≈ -2.3 (see Harris 1996, 2012 update)—provides an excellent fit to the shape of the red side of the PA-48 RGB. This suggests that PA-48 is at least as metal-poor as M92. The implied distance modulus and foreground reddening are $(m-M)_0 = 24.57 \pm 0.11$ and $E(B-V) = 0.08 \pm 0.01$, where the uncertainties are calculated according to the prescription of Mackey et al. (2006, 2007). Our reddening estimate is in good agreement with that predicted by the Schlegel et al. (1998) maps, $E(B-V) = 0.066$, while our distance modulus strongly suggests that PA-48 is a member of the M31 system—it sits at 820^{+43}_{-41} kpc, implying a three-dimensional galactocentric radius of 149^{+19}_{-8} kpc. The PA-48 HB does not extend blueward as far as that of M92. We measure an HB-index $(B-R)/(B+V+R) \approx 0.6$, which may indicate a mild second-parameter effect.

The inset in Figure 2 highlights the fact that stars on the upper RGB of PA-48 span a range in color larger than would be expected if considering only the photometric uncertainties. The registered M92 fiducial suggests that this is driven predominantly by the bluest, and second brightest, of the three most luminous RGB stars (hereafter star-B). Given the potential importance of an RGB color spread, we consider several possibilities that might explain the observed position of star-B on the CMD

1. *Non-member.* Local foreground contamination is moderate—we find 22 stars farther than 20″ from the PA-48 center that are at least as bright as its upper RGB ($m_{\rm F606W} \lesssim 23.5$; Figure 2). However, star-B lies well within the half-light radius of $r_h \approx 6\farcs6$ (see below). The probability that a non-member should fall both within r_h and close to the RGB is very small. The area within r_h is 0.34% of the WFC field of view, while the vicinity of the RGB is, generously, $\approx 1/12$ of the area of the CMD occupied by stars with $m_{\rm F606W} \lesssim 23.5$. Assuming field stars are uniformly distributed on the CCD and the CMD, the chance of one or more falling both within r_h and close to the RGB from 23 trials is just 0.68%. Hence it is very likely that star-B is a member of PA-48.
2. *An internal dispersion in [Fe/H] or age.* In principle, an internal dispersion in [Fe/H] ought to translate into a color spread on the upper RGB, with star-B's blue $m_{\rm F606W} - m_{\rm F814W}$ magnitude indicating a lower abundance than for star-A and star-C. However, stellar evolution models generally indicate that at fixed luminosity the RGB temperature and, hence, broadband color will asymptote to a certain value with decreasing metallicity. To test the sensitivity of $m_{\rm F606W} - m_{\rm F814W}$ color at low [Fe/H], we use isochrones from the Dartmouth Stellar Evolution Database (Dotter et al. 2008). In Figure 3, we plot models with [Fe/H] $= -2.3$ and -2.5, and [α/Fe] $= +0.4$. There is a noticeable shift to the blue with decreasing abundance, but not sufficiently large to match star-B's color. We further computed Dartmouth evolutionary tracks at $0.8 M_\odot$ and [α/Fe] $= +0.4$ for [Fe/H] $= -2.5, -3.0$, and -3.5. On the

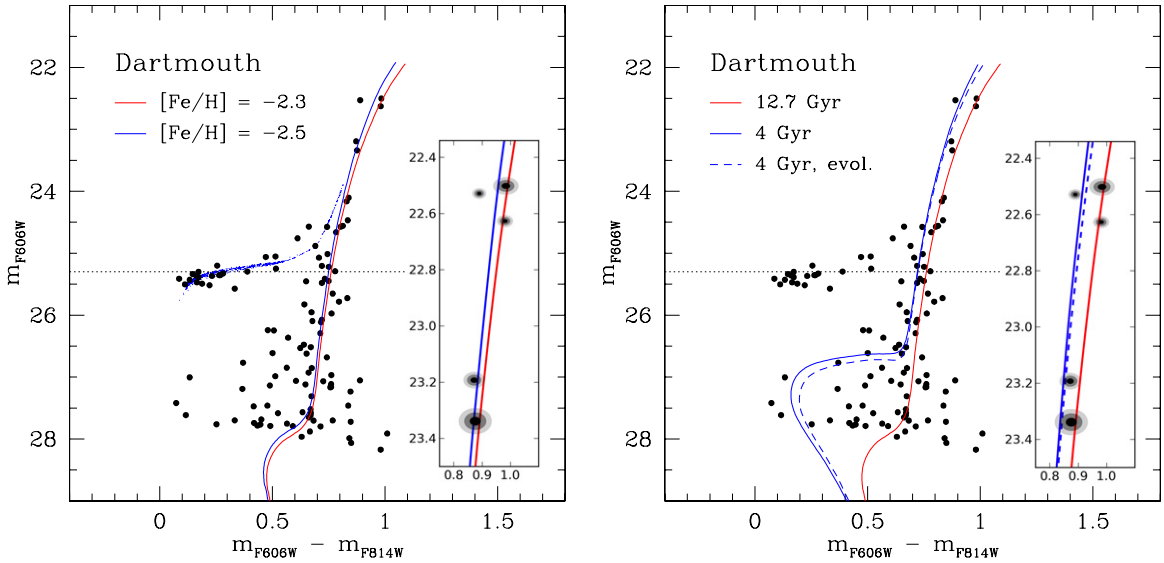

Figure 3. Left panel: the PA-48 CMD with registered Dartmouth isochrones as labeled. Both have [α/Fe] = +0.4. For clarity only the HB for the [Fe/H] = −2.5 model is plotted. Right panel: registered isochrones showing the effects of an internal age dispersion. The first two models have [Fe/H] = −2.3 and [α/Fe] = +0.4; the third "chemically evolved" model has [Fe/H] = −1.9 and [α/Fe] = +0.2.

(A color version of this figure is available in the online journal.)

upper RGB at a luminosity consistent with that of star-B these three models differ in F606W−F814W color by no more than 0.01 mag. Thus, under the assumption of constant [α/Fe], it is unlikely that star-B's position on the CMD is due to it having a much lower [Fe/H] than the bulk of the other stars. However, the insensitivity of $m_{\rm F606W} - m_{\rm F814W}$ color to [Fe/H] at very low abundances also means that we cannot rule out a moderate internal metallicity dispersion in general.

A complicating factor is that our photometry does not reach the ∼13 Gyr main-sequence turnoff; we can only exclude the presence of populations younger than ≈4 Gyr (Figure 3). Decreasing age at fixed composition moves the RGB to the blue; 4 Gyr old stars might nearly match the position of star-B. Mild chemical evolution with age could also be accommodated—as an example we plot a 4 Gyr model with [Fe/H] = −1.9 and [α/Fe] = +0.2.

3. *Asymptotic giant branch (AGB) star.* The time a low-mass star spends ascending the AGB (i.e., before the thermally pulsating phase) is ∼10% of the time it spends in the core He-burning phase. Thus, we may expect to find roughly 1 AGB star for every 10 HB stars in the CMD. In PA-48 we observe ∼17–20 HB stars, consistent with the possibility that star-B is an AGB star. Even so, this object is substantially bluer than all AGB stars visible at comparable brightness in the well-populated CMDs for metal-poor M31 ECs presented by Mackey et al. (2006), which tend to lie much closer to the RGB. It is hence difficult to conclusively assess the viability of this suggestion with only the presently available data; however, in our opinion it remains the most likely option.

3.2. Structure and Luminosity

To quantify the structure of PA-48, we utilized the maximum likelihood algorithm developed by Martin et al. (2008) to study low-luminosity stellar systems. This technique provides robust estimates and uncertainties for parameters such as the half-light radius and ellipticity of an object from resolved photometry. Our

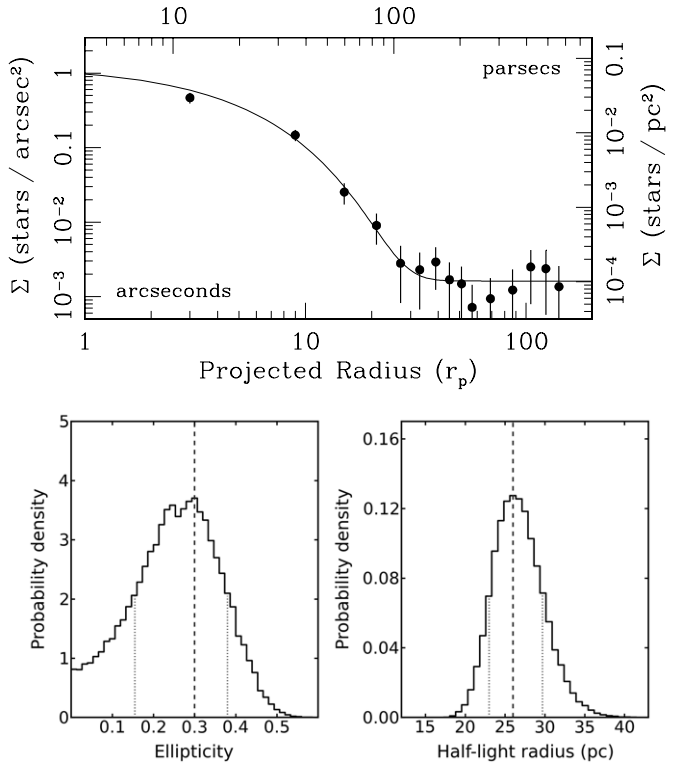

Figure 4. Upper panel: radial surface density profile for PA-48, where the points are the stellar density measured in elliptical annuli and the line represents the best-fitting model found using the algorithm of Martin et al. (2008). Lower panels: marginalized posterior probability distribution functions for the ellipticity and half-light radius of PA-48. The most likely values are indicated with a dashed line; 1σ uncertainties are marked with dotted lines.

results are displayed in Figure 4. The algorithm converges on a unique likelihood maximum, revealing that PA-48 is indeed a moderately elliptical extended object with $\epsilon = 0.30^{+0.08}_{-0.15}$ and $r_h = 6\farcm6^{+0.9}_{-0.8} \approx 26^{+4}_{-3}$ pc. The uncertainties represent 1σ confidence limits; note that there is an additional ±1 pc uncertainty in r_h due to the error in our line-of-sight distance.

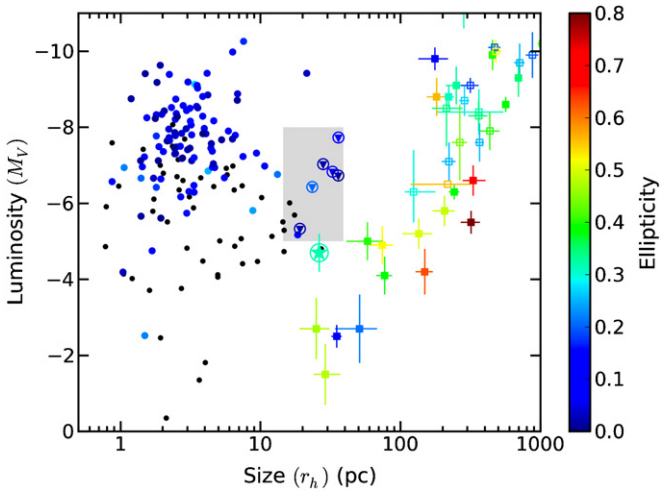

Figure 5. Luminosity vs. size for a variety of stellar systems in the Local Group, color-coded by ellipticity. Filled circles are Galactic globular clusters (Harris 1996); those with no ellipticity measurement are marked in black. Filled (empty) squares are Galactic (M31) dwarf satellites (McConnachie 2012), while circled triangles are M31 ECs (this work). The gray shaded region denotes the approximate area occupied by ECs observed in various Local Group galaxies (e.g., Huxor et al. 2011). PA-48 is marked with a circled star.

(A color version of this figure is available in the online journal.)

A. P. Huxor et al. (2013, in preparation) estimate $M_V \approx -4.7$ for PA-48 from surface photometry of the discovery images. With our resolved measurements we are able to integrate to a larger radius and use a CMD filter to better remove contaminants. The completeness-corrected luminosity we obtain by adding all members down to $m_{\rm F606W} = 27.5$ and within 30′ of the center is $M_V = -4.3$. Experimentation with population synthesis models suggests that for a Kroupa (2001) mass function ≈65% of the total luminosity of the system is included to our faint limit, implying $M_V \approx -4.8$. As per Martin et al. (2008), uncertainties in the total luminosity for systems this faint are dominated by CMD shot noise at a level ±0.5 mag.

4. DISCUSSION

PA-48 is an unusual M31 satellite that is not easily classified. Structurally, it is similar to the faint dwarf companions of the Milky Way as well as the ECs seen around some galaxies in the Local Group. Intriguingly, however, a number of its other characteristics would make it an atypical example of either type of object. To illustrate this point, in Figure 5 we plot a variety of stellar systems on the size–luminosity plane, color-coded by ellipticity. Assessed purely in terms of r_h and M_V, PA-48 appears most akin to the lowest-luminosity Local Group ECs. Although the faintest Milky Way UFDs are of very similar size to PA-48, dwarfs of comparable luminosity to PA-48 have scale radii typically ∼2–3 times larger.

That said, PA-48 appears substantially more elliptical than any Galactic GC measured to date, extended or otherwise, as well as almost all Local Group GCs for which reliable measurements are available (Figure 6 in Huxor et al. 2013). However, it lies comfortably within the range of ellipticities exhibited by faint dwarfs (e.g., Martin et al. 2008; Sand et al. 2012). Unfortunately, few of the low-luminosity diffuse Milky Way GCs have ellipticity measurements in the Harris (1996) catalog. To attempt a fairer comparison, we ran the Martin et al. (2008) software on our *HST* photometry of M31 ECs—three from Mackey et al. (2006),[11] and three from the present program, yet unpublished.[12] These span luminosities $-7.7 \lesssim M_V \lesssim -5.3$ and projected galactocentric radii $15 \lesssim R_{\rm p} \lesssim 115$ kpc. Our results are consistent with the assessment above. Five of the six M31 ECs have $\epsilon < 0.1$ with typical uncertainties of ±0.08, while one (PA-50) has $\epsilon = 0.20 \pm 0.07$, commensurate with the most highly flattened Galactic GCs.

If PA-48 is a cluster then it would also be among the most isolated such objects seen in the Local Group—just one GC of any kind (MGC1 in M31) is known with a larger three-dimensional radius. This appears at odds with its unusually high ellipticity. One might expect that a low-luminosity star cluster with high ellipticity is being tidally disturbed; however, we have strong evidence from MGC1 that tidal forces are exceedingly benign at such large galactocentric distances (Mackey et al. 2010). It may be that PA-48 is on a highly eccentric orbit about M31 and so suffered a disruptive but non-fatal tidal shock some Gyr ago. A radial velocity measurement and orbital modeling will be necessary to determine if this is a viable solution.

As noted above, if PA-48 is a low-luminosity dwarf then it is unusually small in terms of its spatial extent. Comparable systems are observed (Willman 1; Segue 1 and 2) but these are ∼2–3 mag fainter than PA-48. Although the luminosities of such objects can fluctuate substantially with the evolution of their brightest few stars, it is very unlikely that they could get as bright as PA-48 (or vice versa; see Martin et al. 2008); however, the distinction between these systems may not be as great as it appears in Figure 5. Furthermore, only a handful of dwarf galaxies fainter than $M_V = -5$ are known and it is easy to speculate that perhaps the size–luminosity plane is simply not yet sufficiently well sampled to accurately assess how unusual PA-48 would be in this regard. For dwarf galaxies with $M_V \lesssim -8$, where completeness is less of an issue, there is nearly an order of magnitude spread in r_h at given luminosity (e.g., McConnachie 2012).

A key alternative characteristic defining faint dwarfs is an internal spread in [Fe/H]. Unfortunately, we are not able to constrain this possibility for PA-48 given its very metal-poor nature and our choice of broadband filters. Kirby et al. (2011) have shown that UFDs follow the same metallicity–luminosity relation as do the more massive Galactic satellites (their Figure 3). Intriguingly, with $\langle$[Fe/H]$\rangle \lesssim -2.3$ and $\log(L/L_\odot) \approx 3.8$, PA-48 fits closely with this relationship. If PA-48 is a dwarf galaxy then it would be the faintest known example outside the Milky Way. Its isolation would reinforce the possibility that the faintest Galactic UFDs could well exist out to comparable distances, and not be shaped through their interactions with their host.

Finally, it is relevant that PA-48 lies within the thin plane of corotating M31 dwarf galaxies recently identified by Ibata et al. (2013; see also Conn et al. 2013). In this context, knowledge of its radial velocity would be helpful—if PA-48 is a true member of this plane of satellites (PoS) then we expect its velocity to be more negative than the M31 systemic velocity. One might suspect that membership of the M31 PoS would cement PA-48's status as a dwarf galaxy, but this is not clear cut. We do not observe any evidence for M31 GCs being associated with the plane; however, Keller et al. (2012) argue that outer halo

[11] We excluded EC3 ≡ HEC4 due to heavy field contamination.
[12] PA-2, PA-12, and PA-50.

Milky Way GCs *are* members of the Galactic PoS defined by, e.g., Metz et al. (2009).

A.D.M. and G.F.L. are grateful for support from the Australian Research Council (Discovery Projects DP1093431 and DP110100678, and Future Fellowship FT100100268).

Facility: HST

REFERENCES

Anderson, J., & Bedin, L. R. 2010, PASP, 122, 1035
Belokurov, V., Zucker, D. B., Evans, N. W., et al. 2007, ApJ, 654, 897
Brown, T. M., Ferguson, H. C., Smith, Ed., et al. 2005, AJ, 130, 1693
Brown, T. M., Tumlinson, J., Geha, M., et al. 2012, ApJL, 753, L21
Collins, M. L. M., Chapman, S. C., Irwin, M., et al. 2009, MNRAS, 396, 1619
Conn, A. R., Lewis, G. F., Ibata, R. A., et al. 2013, ApJ, 766, 120
Da Costa, G. S., Grebel, E. K., Jerjen, H., Rejkuba, M., & Sharina, M. E. 2009, AJ, 137, 4361
Dolphin, A. E. 2000, PASP, 112, 1383
Dotter, A., Chaboyer, B., Jevemović, D., et al. 2008, ApJS, 178, 89
Galleti, S., Federici, L., Bellazzini, M., Fusi Pecci, F., & Macrina, S. 2004, A&A, 416, 917
Harris, W. E. 1996, AJ, 112, 1487
Huxor, A. P., Ferguson, A. M. N., Barker, M. K., et al. 2009, ApJL, 698, L77
Huxor, A. P., Ferguson, A. M. N., Tanvir, N. R., et al. 2011, MNRAS, 414, 770
Huxor, A. P., Ferguson, A. M. N., Veljanoski, J., Mackey, A. D., & Tanvir, N. R. 2013, MNRAS, 429, 1039
Huxor, A. P., Tanvir, N. R., Ferguson, A. M. N., et al. 2008, MNRAS, 385, 1989
Huxor, A. P., Tanvir, N. R., Irwin, M. J., et al. 2005, MNRAS, 360, 1007
Hwang, N., Lee, M. G., Lee, J. C., et al. 2011, ApJ, 738, 58
Ibata, R. A., Lewis, G. F., Conn, A. R., et al. 2013, Natur, 493, 62
Keller, S. C., Mackey, A. D., & Da Costa, G. S. 2012, ApJ, 744, 57
Kirby, E. N., Lanfranchi, G. A., Simon, J. D., Cohen, J. G., & Guhathakurta, P. 2011, ApJ, 727, 78
Kirby, E. N., Simon, J. D., Geha, M., Guhathakurta, P., & Frebel, A. 2008, ApJ, 682, 1217
Koposov, S. E., Yoo, J., Rix, H.-W., et al. 2009, ApJ, 696, 2179
Kroupa, P. 2001, MNRAS, 322, 231
Leaman, R. 2012, AJ, 144, 183
Mackey, A. D., Ferguson, A. M. N., Irwin, M. J., et al. 2010, MNRAS, 401, 533
Mackey, A. D., Huxor, A., Ferguson, A. M. N., et al. 2006, ApJL, 653, L105
Mackey, A. D., Huxor, A., Ferguson, A. M. N., et al. 2007, ApJL, 655, L85
Martin, N. F., de Jong, J. T. A., & Rix, H.-W. 2008, ApJ, 684, 1075
Martin, N. F., Ibata, R. A., Chapman, S. C., Irwin, M., & Lewis, G. F. 2007, MNRAS, 380, 281
McConnachie, A. W. 2012, AJ, 144, 4
McConnachie, A. W., & Côté, P. 2010, ApJL, 722, L209
McConnachie, A. W., Huxor, A., Martin, N. F., et al. 2008, ApJ, 688, 1009
McConnachie, A. W., Irwin, M. J., Ibata, R. A., et al. 2009, Natur, 461, 66
Metz, M., Kroupa, P., & Jerjen, H. 2009, MNRAS, 394, 2223
Norris, J. E., Yong, D., Gilmore, G. F., & Wyse, R. F. G. 2010, ApJ, 711, 350
Richardson, J. C., Irwin, M. J., McConnachie, A. W., et al. 2011, ApJ, 732, 76
Sand, D. J., Strader, J., Willman, B., et al. 2012, ApJ, 756, 79
Schlegel, D. J., Finkbeiner, D. P., & Davis, M. 1998, ApJ, 500, 525
Simon, J. D., & Geha, M. 2007, ApJ, 670, 313
Simon, J. D., Geha, M., Minor, Q. E., et al. 2011, ApJ, 733, 46
Sirianni, M., Jee, M. J., Benítez, N., et al. 2005, PASP, 117, 1049
Stonkutė, R., Vansevičius, V., Arimoto, N., et al. 2008, AJ, 135, 1482
Tanvir, N. R., Mackey, A. D., Ferguson, A. M. N., et al. 2012, MNRAS, 422, 162
Willman, B., Blanton, M. R., West, A. A., et al. 2005, AJ, 129, 2692
Zucker, D. B., Belokurov, V., Evans, N. W., et al. 2006, ApJL, 650, L41